Science Advances
AAAS

Supplementary Materials for

RGS12 polarizes the GPSM2-GNAI complex to organize and elongate stereocilia in sensory hair cells

Anil Akturk *et al.*

Corresponding author: Basile Tarchini, basile.tarchini@jax.org

Sci. Adv. **8**, eabq2826 (2022)
DOI: 10.1126/sciadv.abq2826

The PDF file includes:

Figs. S1 to S8

Other Supplementary Material for this manuscript includes the following:

Data source file S1

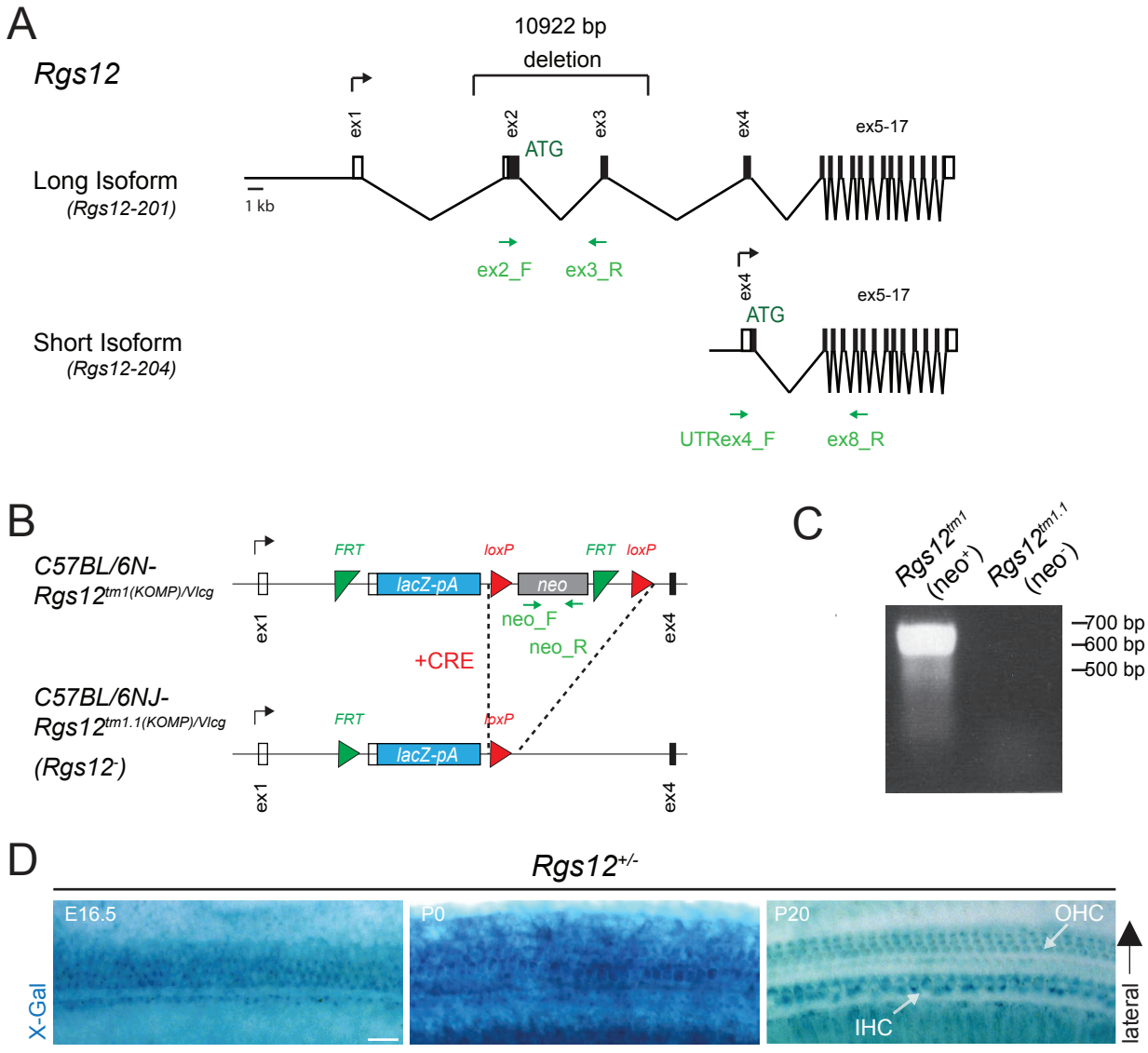

Supplementary Figure 1

Supplementary figure 1. *Rgs12* loss-of-function mouse model used in this study. A) Diagram of two main *Rgs12* transcripts described previously. Exon notation is for the full-length (long) isoform (ENSMUST00000030984.14; Rgs12-201), and the downstream start site for the shorter isoform used in Fig. 6C (ENSMUST00000114281.8; Rgs12-204) is also indicated. The 10,922bp deletion in the *tm1(KOMP)/Vlcg* mutant allele (B) removes the first coding exon (exon 2) and exon 3. Coding exons are in black. **B)** Diagram of the *Rgs12* genomic insertion before (top; *tm1(KOMP)/Vlcg* allele) and after (bottom; *tm1.1(KOMP)/Vlcg* allele) CMV-Cre-mediated recombination to excise the neomycin-resistance (neo) selection cassette. $Rgs12^{tm1.1(KOMP)/Vlcg}$ ($Rgs12^{-}$) is the allele used throughout the study. **C)** 2% agarose gel showing the loss of a neo PCR product after Cre recombination. **D)** Surface views of the $Rgs12^{+/-}$ auditory epithelium following X-Gal chemistry to reveal *LacZ* expression (whole-mount of the cochlear base). *Rgs12* is broadly expressed in the cochlear floor at E16.5, P0 and P20, but enriched at higher level in sensory HCs (arrows). OHC, outer HC; IHC, inner HC. Scale bar 20µm (D).

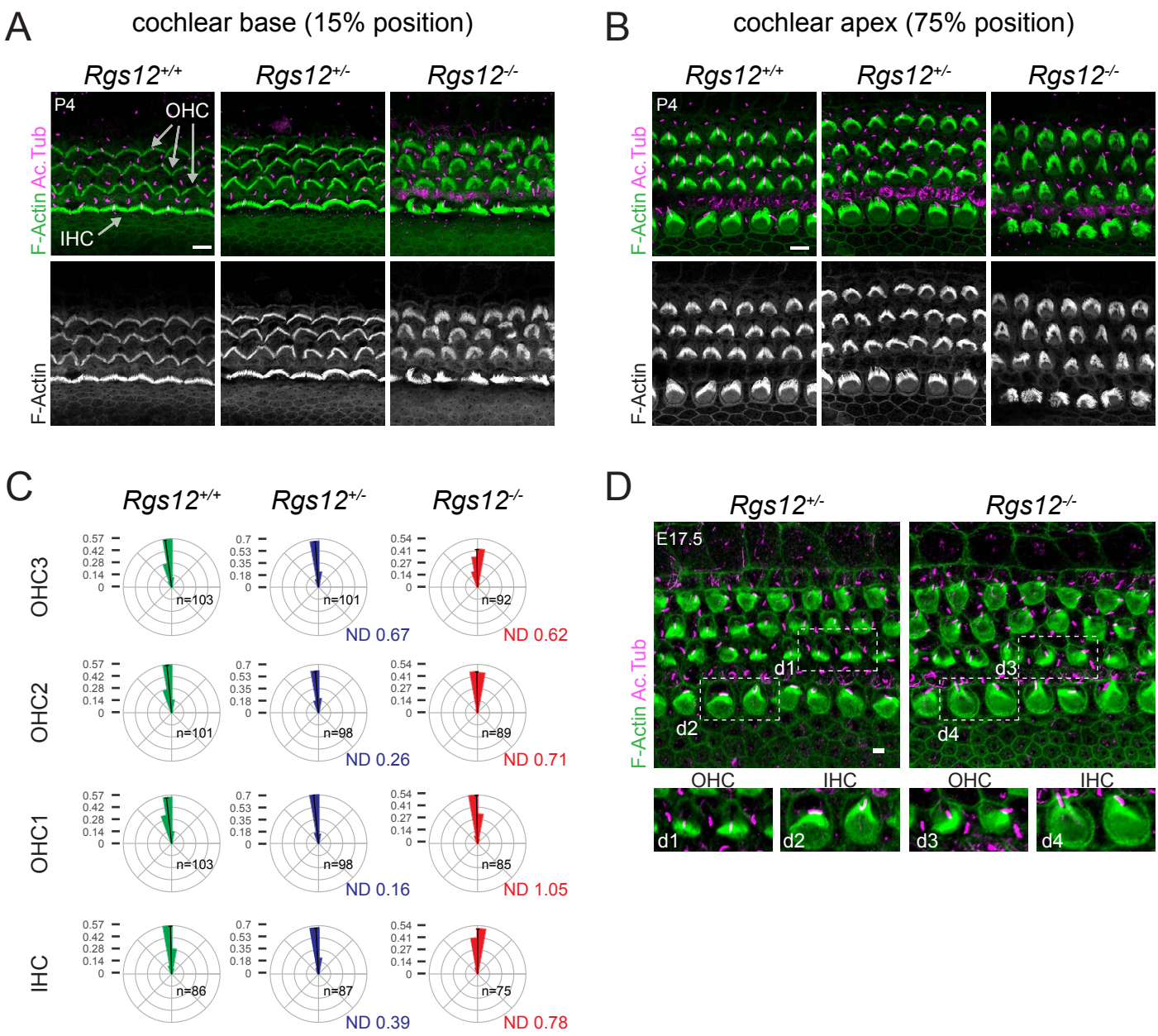

Supplementary Figure 2

Supplementary figure 2. Defective hair bundle morphogenesis but proper HC orientation in *Rgs12* mutants. A-B) Surface views of the P4 auditory epithelium at the cochlear base (A, 15% cochlear position) and apex (B, 75%). F-actin is labeled with phalloidin and acetylated tubulin (Ac.Tub) is immunolabeled to reveal primary cilia/HC kinocilia. OHC, outer HC; IHC, inner HC. The middle-turn cochlear position (50%) is shown in Fig. 2A. *Rgs12*$^{-/-}$ HCs, but not *Rgs12*$^{+/-}$ HCs, show severely dysmorphic hair bundles compare to a wild-type control (*Rgs12*$^{+/+}$). **C)** P4 HC orientation based on the position of the kinocilium. Circular histograms indicate frequency distribution of HC orientation at the cochlear middle-turn (10° bins in a referential where 90° (noon) is lateral and 0° (3 o'clock) is towards the cochlear base). HCs analyzed (n) represent N=3 animals. Black lines and terminal arcs indicate circular mean (line orientation) and circular standard deviation (arc length), respectively (values indicated in Data Source File S1). Normalized difference (ND) values indicate how many standard deviations separate the circular means using *Rgs12*$^{+/+}$ as reference. *Rgs12* mutants do not show HC orientation defects. **D)** Acetylated tubulin and F-actin labeling at the E17.5 base. Boxed regions are magnified at the bottom. Scale bars 5µm (A-B), 4µm (D).

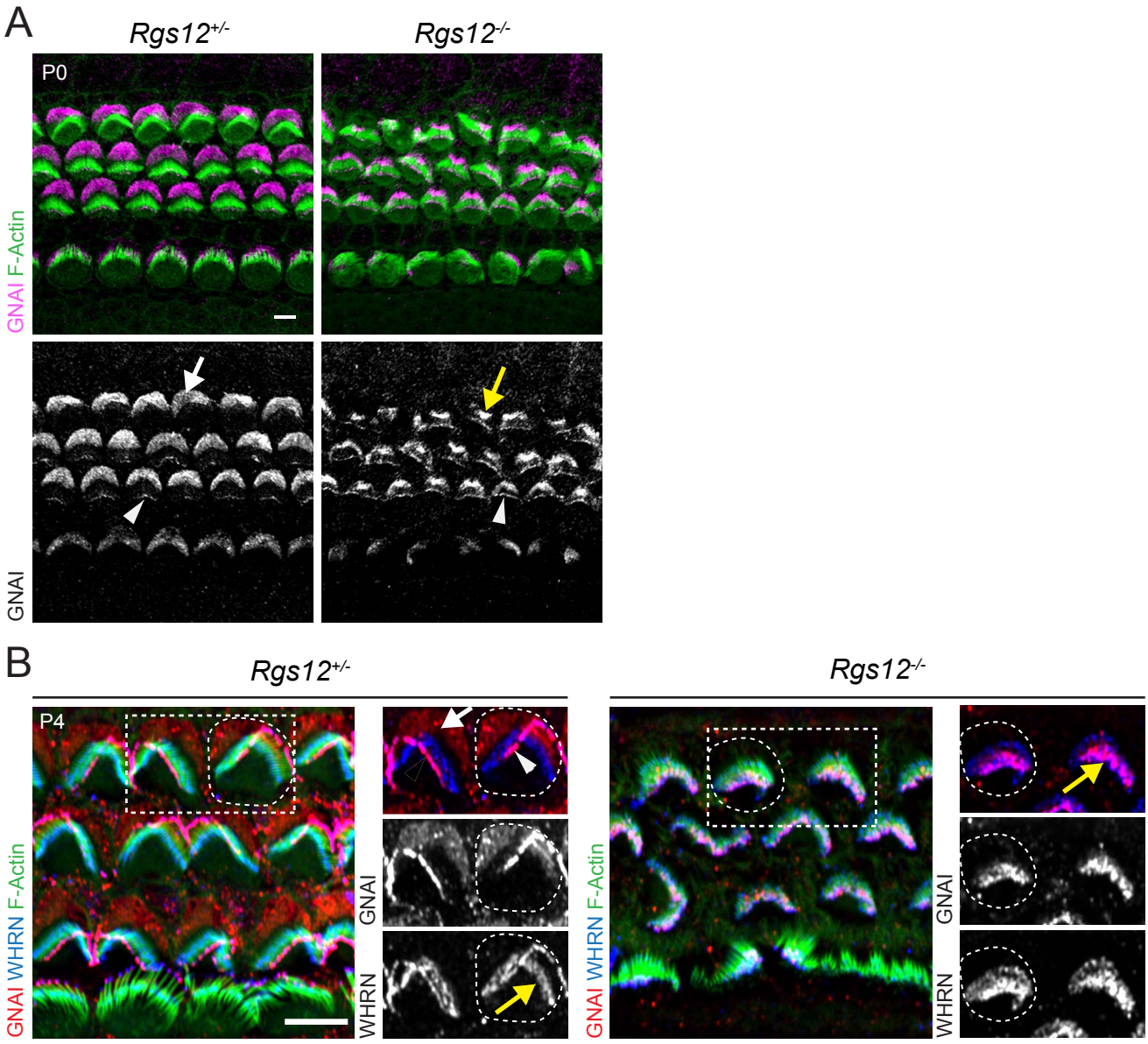

Supplementary Figure 3

Supplementary figure 3. GNAI delocalization in absence in RGS12. A) GNAI immunolabeling at the P0 cochlear base. GNAI enrichment at the bare zone (arrow) is absent in *Rgs12* mutants, where GNAI is instead concentrated near row 1 stereocilia (yellow arrow). Arrowheads indicate GNAI signal at stereocilia tips. **B)** GNAI and WHRN co-immunolabeling at the P4 middle-turn. In controls (left), WHRN signals coincide with GNAI at stereocilia tips (arrowheads). WHRN also labels the base of stereocilia (yellow arrow) whereas GNAI labels the bare zone (white arrow). In *Rgs12* mutants (right), GNAI matches WHRN signals at the hair bundle position (yellow arrow), and GNAI is absent at the bare zone. Boxed OHCs are magnified to the right. The apical circumference of one OHC is outlined in B. Scale bars 5µm.

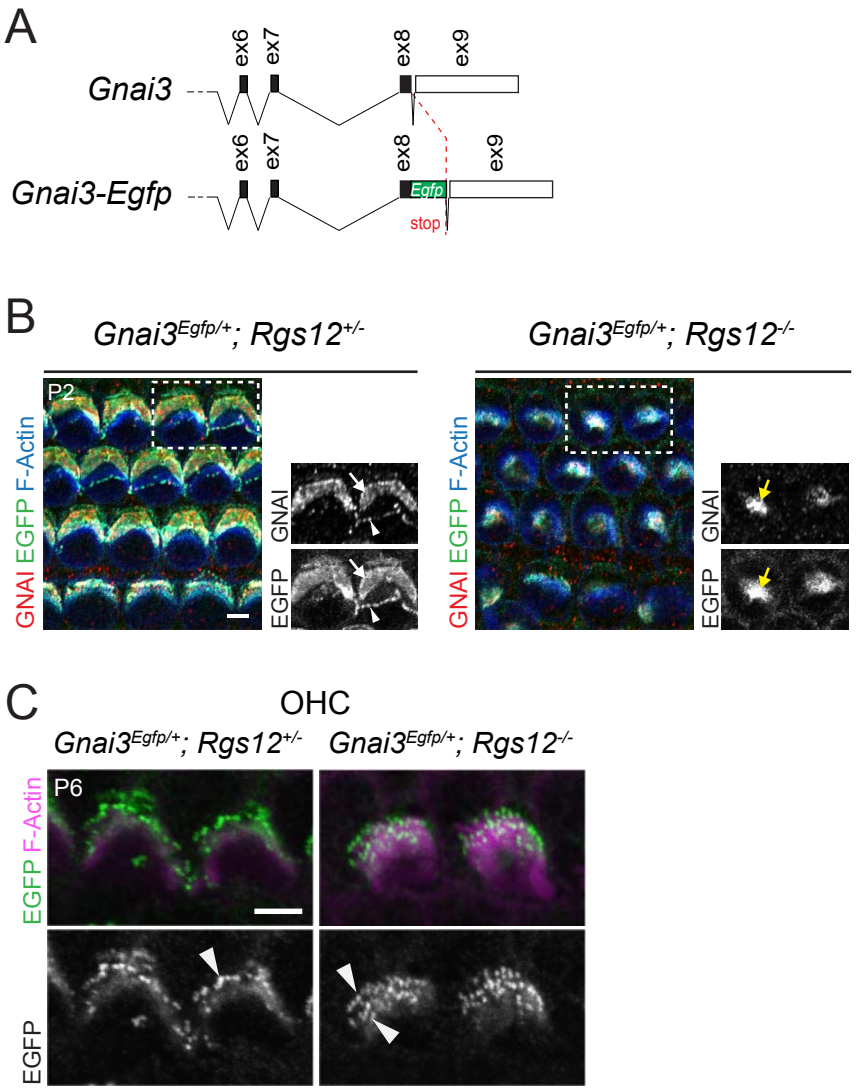

Supplementary Figure 4

Supplementary figure 4. *Gnai3-Egfp* knock-in mouse model and GNAI3-EGFP signals in *Rgs12* mutants. A) Diagram of the *Gnai3-Egfp* knock-in mouse model generated in this study. *Egfp* was inserted in frame C-terminal to *Gnai3* coding sequence in exon 8, followed by a stop codon. Coding exons are shown in black. **B)** EGFP and GNAI co-labeling in P2 $Gnai3^{Egfp/+}$; $Rgs12^{+/-}$ controls and $Gnai3^{Egfp/+}$; $Rgs12^{-/-}$ mutants at the middle-turn. GNAI and EGFP signals coincide at the bare zone (arrows) and at stereocilia tips (arrowheads) in control HCs (left). Their aberrant enrichment at the position of the hair bundle also coincides in mutant HCs (right; yellow arrows). Boxed regions are shown as single channel views to the right. **C)** EGFP signals in $Gnai3^{Egfp/+}$; $Rgs12^{+/-}$ controls and $Gnai3^{Egfp/+}$; $Rgs12^{-/-}$ mutant OHCs at the P6 base. Signals at stereocilia tips (arrowheads) encompasses all rows in mutants. Scale bars 5µm.

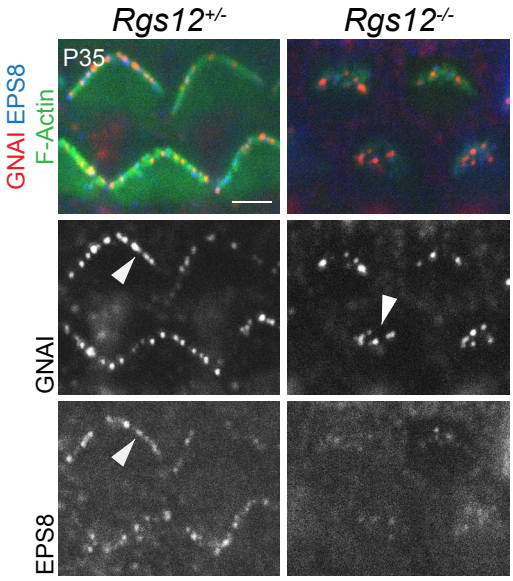

Supplementary Figure 5

Supplementary figure 5. Adult hair bundle defects in absence of RGS12. GNAI and EPS8 co-immunolabeling in P35 OHCs at the middle-turn. GNAI and EPS8 colocalize at stereocilia tips (arrowheads). GNAI is still observed at tips in very dysmorphic OHC bundles. Scale bar 5µm.

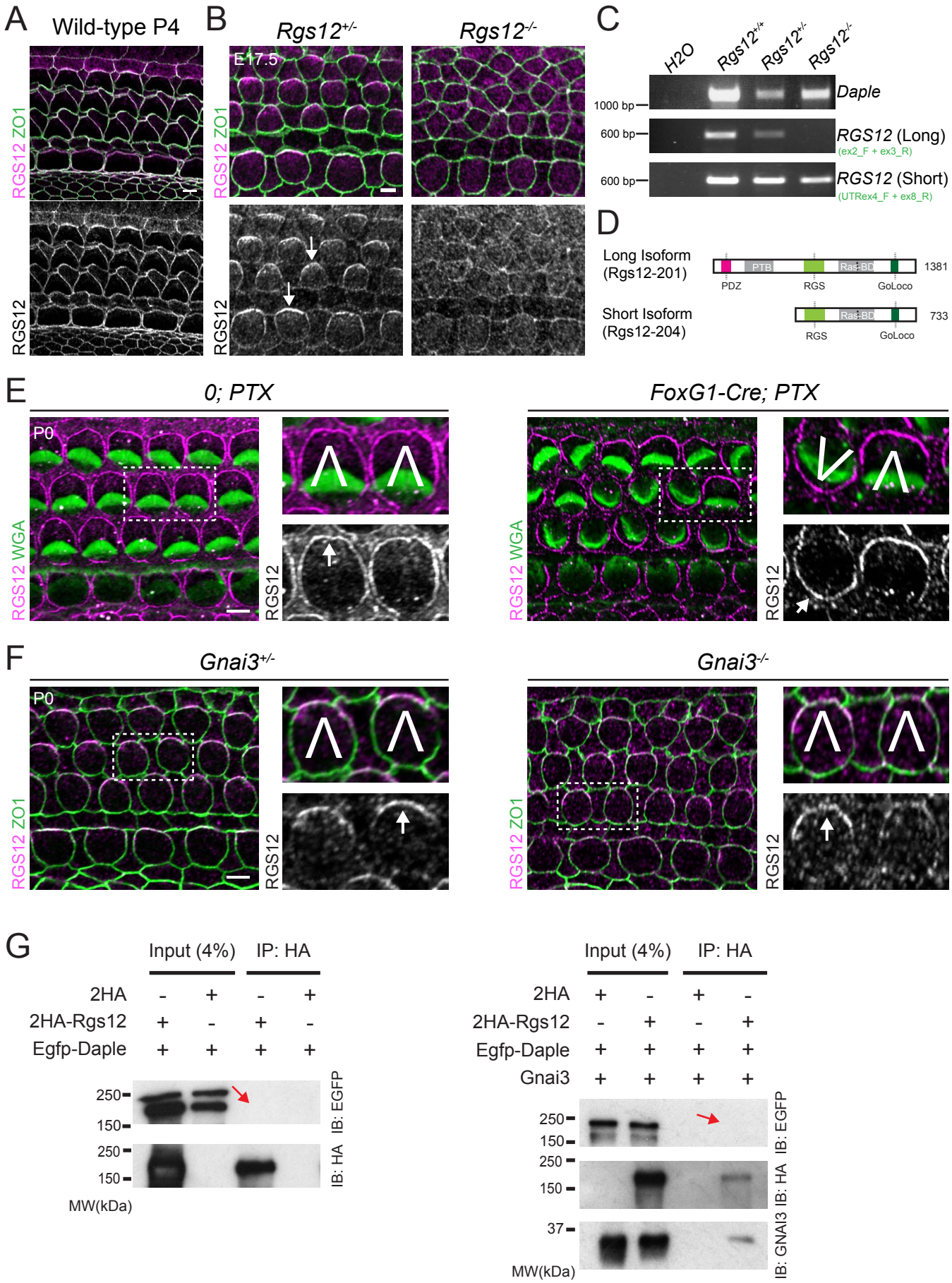

Supplementary Figure 6

Supplementary figure 6. RGS12 protein localization in hair cells, *Rgs12* isoform expression in *Rgs12*$^{-/-}$ mutants and absence of binding between RGS12 and DAPLE. A) RGS12 immunolabeling at the P4 base with ZO1 as junctional marker. RGS12 is not obviously planar polarized at P4 HC junctions unlike at earlier stages (see Fig. 6A-B). **B)** RGS12 immunolabeling at the E17.5 cochlear base. Lateral junction enrichment in controls (arrows) is absent in *Rgs12* mutants. Remaining signals in *Rgs12*$^{-/-}$ may correspond to the RGS12 short (S) isoform that is still expressed (C), but not polarized (Fig. 6C). **C)** RT-PCRs to amplify *Daple* and *Rgs12* long (full length) and short isoforms in P0 cDNA preparations of the cochlear floor for the *Rgs12* genotypes indicated. Primers used are labeled in green and depicted in Fig. S1A. Note how the transcript producing the long isoform is missing in *Rgs12*$^{-/-}$ mutants, but a transcript specific for the short isoform is retained, as expected from the position of its transcriptional start site downstream of the *Rgs12*$^{-}$ deletion (see Fig. S1A). **D)** Diagram of RGS12 long (full length) and short isoforms with their main functional motifs. **E)** RGS12 immunolabeling at P0 at the middle-turn with Wheat Germ Agglutinin (WGA) to label hair bundles. Polarized junctional RGS12 signals are retained in HCs expressing Pertussis toxin catalytic subunit (PTXa) under the control of *FoxG1-Cre*. PTXa disrupts the GPSM2-GNAI complex and hair bundle morphogenesis, but also the EMX2-GPR156-GNAI signaling cascade and HC orientation (*57*). This explains why RGS12 junctional crescents (arrows) follow the apical cytoskeleton in misoriented OHCs. "V" vectors indicate HC orientation based on the shape of the hair bundle. Boxed OHCs are magnified to the right. Controls lack the *FoxG1-Cre* driver ("0"). **F)** RGS12 immunolabeling at the P0 middle-turn. RGS12 polarized distribution at the lateral junction is unaffected in absence of GNAI3. **G)** EGFP-DAPLE does not co-immunoprecipitate with 2HA-RGS12 in HEK293 cell extracts. HEK293 cells were co-transfected with the constructs indicated, followed by HA immunoprecipitation. EGFP-DAPLE is not detected on IP blots (red arrows), even when untagged Gnai3 is co-transfected with 2HA-Rgs12 and Egfp-Daple (right panels). MW, molecular weight in kiloDalton (kDa). IP, immunoprecipitation. IB, immunoblot antibody. Scale bars 5µm.

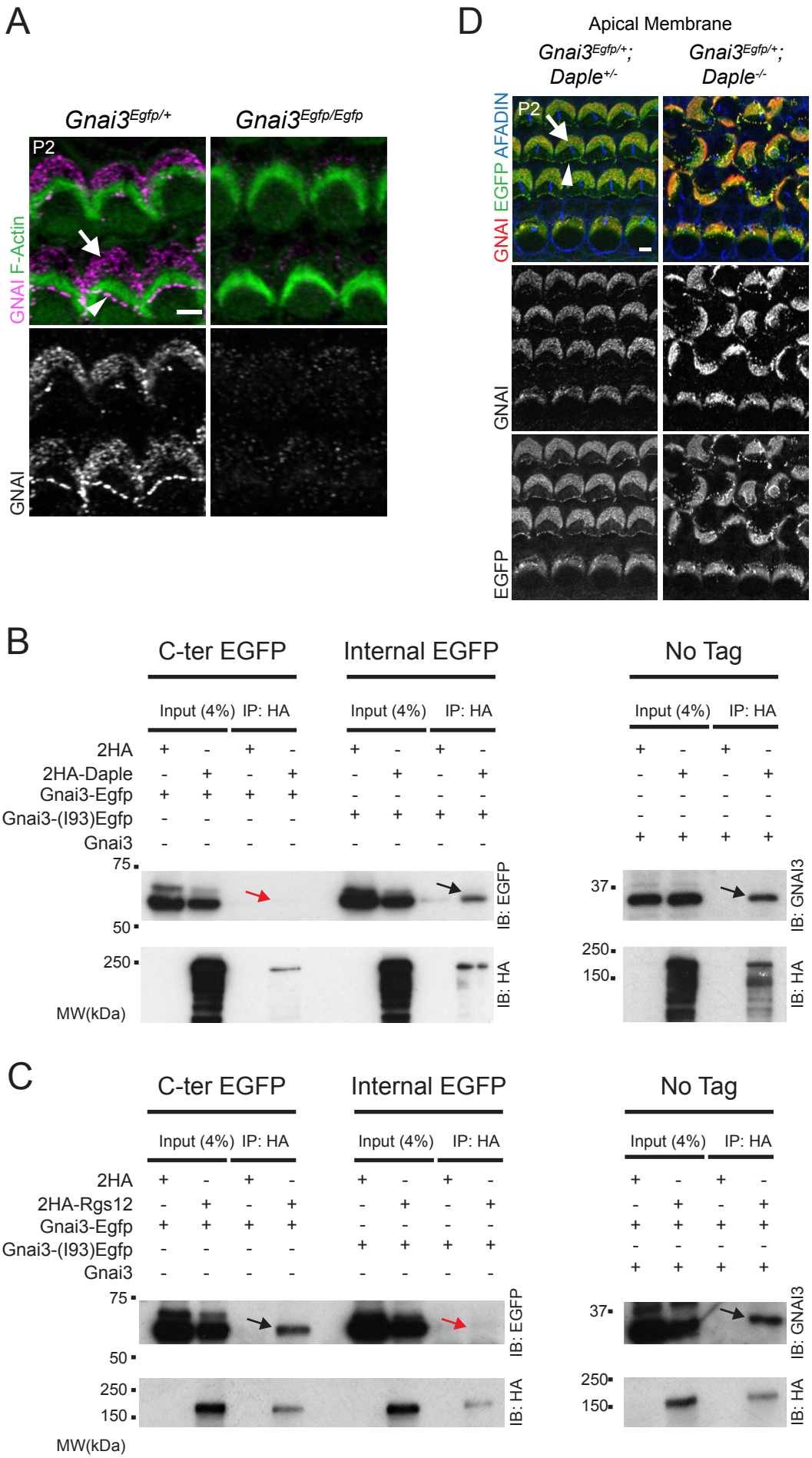

Supplementary Figure 7

Supplementary figure 7. GNAI3-EGFP localization and binding to 2HA-RGS12 but not 2HA-DAPLE in HEK293 cells. **A)** GNAI immunolabeling at the middle-turn using the Santa Cruz Biotechnology antibody sc-262. In *Gnai3*$^{Egfp/+}$, sc-262 labels the bare zone (arrow) and stereocilia tips (arrowhead). In *Gnai3*$^{Egfp/Egfp}$ homozygotes, sc-262 signals are very weak, likely because sc-262 raised against a C-terminal region of GNAI3 does not detect efficiently the GNAI3-EGFP fusion. **B)** Representative example for Fig. 7F showing immunoprecipitation of various GNAI3 species with 2HA and 2HA-DAPLE in HEK293 cell extracts. HEK293 cells were co-transfected with the constructs indicated, followed by HA immunoprecipitation. Untagged GNAI3 (right) or internal EGFP-tagged GNAI3 (GNAI3-(I93)EGFP; center) are co-immunoprecipitated with 2HA-DAPLE (black arrows), but C-terminal EGFP prevents GNAI3-EGFP co-immunoprecipitation (red arrow). 3 independent experiments were quantified to produce the graph in Fig. 7F (see Data Source File S1). **C)** Immunoprecipitation of various GNAI3 species with 2HA and 2HA-RGS12 in HEK293 cell extracts. HEK293 cells were co-transfected with the constructs indicated, followed by HA immunoprecipitation. Untagged GNAI3 (right) or C-terminal EGFP-tagged GNAI3 (GNAI3-EGFP; left) are co-immunoprecipitated with 2HA-RGS12 (black arrows). Internal EGFP prevents GNAI3-(I93)EGFP co-immunoprecipitation (red arrow). This outcome was observed in 3 independent experiments. **D)** GNAI immunolabeling with EGFP signals at the apical membrane level in P2 *Gnai3*$^{Egfp/+}$*; Daple*$^{+/-}$ controls and *Gnai3*$^{Egfp/+}$*; Daple*$^{-/-}$ mutants. GNAI3-EGFP polarization at the bare zone (arrow) is disrupted in absence of DAPLE. The Afadin antibody labels apical junctions but also primary cilia and hair cell kinocilia. MW, molecular weight in kiloDalton (kDa). IP, immunoprecipitation. IB, immunoblot antibody. Scale bars 5µm.

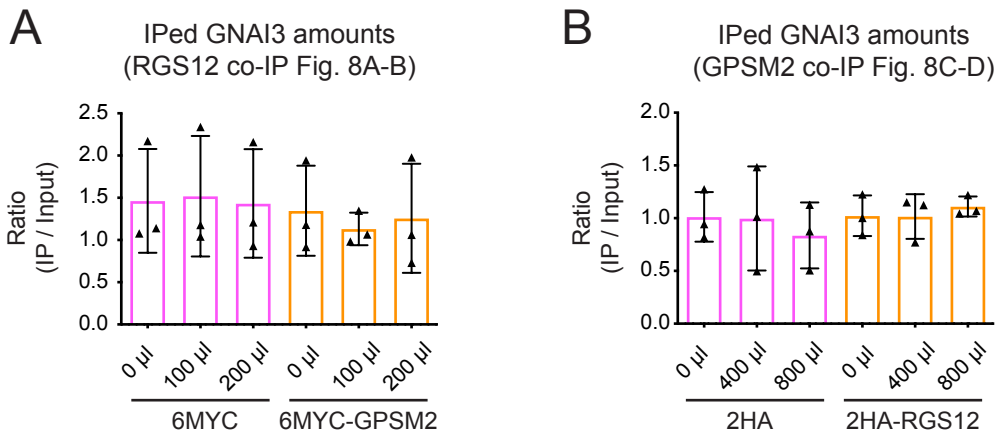

Supplementary Figure 8

Supplementary figure 8. Quantification of GNAI3-EGFP amounts immunoprecipitated in Figure 7A-D. A-B) GNAI3-EGFP amounts immunoprecipitated in 2HA-RGS12 co-immunoprecipitation experiments (A; refers to Fig. 8A-B) and in MYC-GPMS2 co-immunoprecipitation experiments (B; refers to Fig. 8C-D). The quantification verifies that similar GNAI3-EGFP amounts are immunoprecipitated across conditions. IP band intensity (ratio of input). Mean±SD for 3 experiments. One-way Anova with Tukey's multiple comparisons. A: 6myc vs 6myc-Gpsm2: ns p=0.9998 (0 µl), p= 0.9592 (100µl), p=0.9989 (200µl). B: 2HA vs 2HA-RGS12: ns p>0.9999 (0µl, 400µl), p=0.8385 (800µl).